*University of Thi-Qar Journal of agricultural research*

*Thi-Qar Journal of agricultural research*

*ISSN Onlin:2708-9347, ISSN Print: 2708-9339 Volume 15, Issue 1 (2026) PP 229-242*

*https://jam.utq.edu.iq/index.php/main* https://doi.org/10.54174/0kgmcw24

# RGB Image-Based Proxy Assessment of Soil Inversion, Fragmentation, and Surface Structural Roughness After Three-Body Moldboard Ploughing: A Pilot Study

[1]Rawaz Jalal Hama Ali, [2]Fawzy Faidhullah Khurshid, [3]Shaee Adeeb Ghareeb

[!,2,3]Department of Biotechnology and Crop Science, College of Agricultural Engineering Sciences, University of Sulaimani, Kurdistan-Iraq

*E-mail: Rawaz.hamaali@univsul.edu.iq*

*E-mail Fawzy.khurshid@univsul.edu.iq*

*E-mail Shaee.gharib@univsul.edu.iq*

## Abstract

This pilot study developed and tested a low-cost RGB image-processing workflow for assessing post-plough soil surface condition after three-body mouldboard ploughing. The study focused on deriving image-based proxy indicators of visible vegetation exposure, relative clod-size distribution, and surface structural roughness. Ten field images were captured at the College of Agricultural Engineering, Bakrajo, University of Sulaimani, Kurdistan Region, Iraq, using a Samsung Galaxy S24 Ultra smartphone camera. Visible vegetation exposure was estimated using HSV color segmentation. Soil clod features were extracted using grayscale conversion, Gaussian smoothing, Canny edge detection, and contour analysis. Surface structural roughness was estimated using an edge-density index. Results showed a mean visible vegetation exposure of approximately 1.96%, suggesting effective apparent soil inversion within the analyzed images. The mean image-derived median clod diameter was approximately 17.06 pixels, with relative clod classes dominated by fine and medium categories. The mean edge-density roughness index was approximately 0.301, indicating a highly textured post-plough surface typical of primary tillage. The proposed workflow should be interpreted as a comparative proxy-assessment method rather than a replacement for calibrated physical measurements such as sieve analysis, profilometry, LiDAR, or photogrammetric 3D reconstruction. The study demonstrates the potential of simple RGB imagery for rapid field-level tillage assessment and provides a foundation for future calibrated validation and low-cost drone-based monitoring.

***Keywords:*** **moldboard plough, RGB image processing, soil inversion, tillage assessment and precision agriculture.**

## I. INTRODUCTION

Tillage is a fundamental agricultural operation that influences soil structure, residue incorporation, soil aeration, water movement, weed control, and seedbed preparation. Among primary tillage implements, the mouldboard plough remains widely used because of its ability to cut, lift, and invert soil slices. The quality of mouldboard ploughing is influenced by implement geometry, working depth, forward speed, soil condition, and soil-tool interaction (Koolen & Kuipers, 1983; Godwin, 2007; Godwin et al., 2007). Because mouldboard ploughing modifies both the vertical and horizontal arrangement of soil, its performance should be evaluated using more than one surface indicator.

The quality of post-plough soil condition cannot be judged by inversion alone. Effective inversion may bury visible vegetation and residues, but it may still leave a rough surface with medium or large clods. Soil fragmentation depends on soil moisture,

*University of Thi-Qar Journal of agricultural research*

*Thi-Qar Journal of agricultural research*

*ISSN Onlin:2708-9347, ISSN Print: 2708-9339 Volume 15, Issue 1 (2026) PP 229-242*

*https://jam.utq.edu.iq/index.php/main* https://doi.org/10.54174/0kgmcw24

texture, cohesion, organic matter, working depth, and implement adjustment. Therefore, post-tillage assessment should consider soil inversion, clod-size distribution, and surface roughness together rather than as isolated indicators (Koolen & Kuipers, 1983; Spoor, 2006; Godwin, 2007).

Traditional evaluation of soil cloddiness and roughness often relies on manual inspection, clod measurement, sieve analysis, pin meters, profilometers, laser scanning, or other specialized measurement devices. These methods can provide stronger physical measurements, but they are time-consuming, labor-intensive, and difficult to repeat frequently under ordinary field conditions (Huang & Bradford, 1992; Darboux & Huang, 2003; Jester & Klik, 2005). Soil surface roughness is especially important because it affects infiltration, runoff, erosion, evaporation, seed placement, and machinery performance (Bögel et al., 2016; Dusséaux & Vannier, 2022). However, accurate roughness measurement generally requires physical elevation data or 3D reconstruction, not only 2D visual interpretation.

Recent developments in image processing, photogrammetry, stereo vision, and drone-based imaging have created new opportunities for rapid soil surface assessment. Image-based reconstruction methods can estimate soil surface roughness and microtopography from overlapping images or 3D point clouds (Eltner et al., 2016; Gilliot et al., 2017; Azizi et al., 2021). Close-range photogrammetry has also been applied to evaluate post-tillage soil structure quantitatively

At the same time, simpler RGB image-processing methods remain valuable for low-cost and field-accessible assessment. Earlier work demonstrated the possibility of using image processing for soil tilth or aggregate-size analysis (Bogrekci & Godwin, 2007), while recent studies have used UAV imagery for crop residue and surface-cover estimation (Upadhyay et al., 2022; Azimi et al., 2024). These developments suggest that ordinary field images may support practical proxy indicators, even when full physical calibration is not available.

There remains a practical need for a simple, low-cost, field-applicable workflow that can use standard RGB images to assess post-plough soil condition. Such a method would not replace sieve analysis, profilometry, LiDAR, stereo vision, or photogrammetric 3D reconstruction. Instead, it could provide rapid comparative proxy indicators for teaching, field monitoring, machinery adjustment, and preliminary research.

This pilot study develops and tests a low-cost RGB image-processing workflow for deriving proxy indicators of visible vegetation exposure, relative clod-size distribution, and edge-density surface structural roughness after three-body mouldboard ploughing. The workflow is also positioned as a foundation for future low-cost drone or UAV-based tillage assessment, where the same image-processing logic could be applied to larger field areas using nadir RGB imagery.

*1.1 Objective*

The objective of this pilot study was to develop and test a low-cost RGB image-processing workflow for deriving proxy indicators of soil inversion, clod fragmentation, and surface structural roughness following three-body mouldboard ploughing under field conditions.

*1.2 Research question*

Can RGB image-based analysis provide reproducible and operationally meaningful proxy indicators for evaluating post-plough soil surface condition?

*1.3 Hypothesis*

It was hypothesized that image-derived proxy indicators of visible vegetation exposure, relative clod-size distribution, and edge-based roughness can reflect post-plough soil surface condition and provide useful information about mouldboard plough performance.

*University of Thi-Qar Journal of agricultural research*

*Thi-Qar Journal of agricultural research*

*ISSN Onlin:2708-9347, ISSN Print: 2708-9339 Volume 15, Issue 1 (2026) PP 229-242*

*https://jam.utq.edu.iq/index.php/main* https://doi.org/10.54174/0kgmcw24

## II. MATERIALS AND METHODS

*2.1 Study design*

This study was designed as a pilot observational quantitative study based on RGB image analysis of post-plough soil surfaces. The study did not aim to replace conventional physical measurements such as sieve analysis, profilometry, LiDAR, stereo vision, or photogrammetric 3D reconstruction. Instead, it aimed to test whether low-cost RGB images could generate practical proxy indicators for comparative assessment of mouldboard ploughing quality. This distinction is important because physical soil roughness and clod-size measurement usually require calibrated reference methods or 3D surface information (Jester & Klik, 2005; Gilliot et al., 2017; Azizi et al., 2021).

*2.2 Study site*

Images were collected from a ploughed field at the College of Agricultural Engineering, Bakrajo, University of Sulaimani, Kurdistan Region, Iraq. The approximate geographic coordinates of the study site were 35°32'07.9"N, 45°21'52.1"E, equivalent to approximately 35.5355°N, 45.3645°E. The site was selected because it contained visible post-plough soil surface patterns created by a three-body mouldboard plough, including soil inversion features, clod formation, exposed vegetation patches, and surface irregularity. A pre-plough reference images showed visible green vegetation coverage of 15.83%.

*2.3 Image acquisition*

Field images were captured after ploughing using a Samsung Galaxy S24 Ultra smartphone camera. A total of ten Ultra High Quality RGB images were selected for analysis. The selected images represented visible variation in post-plough soil surface condition, including vegetation exposure, clod structure, and roughness. Images were captured at close range to improve visibility of soil aggregates and texture.

*2.4 Image-processing environment*

All image-processing tasks were conducted using a Python-based workflow in a Google Colab/OpenCV environment. OpenCV was used for image processing because it is a widely used open-source computer-vision library for extracting and processing visual data (Bradski, 2000). NumPy was used for numerical operations, Pandas for tabular data handling, and Matplotlib for visualization. Fixed processing parameters were applied consistently across the images to improve repeatability.

*2.5 Image-derived variables*

Three proxy variables were extracted from each image: Visible Vegetation Exposure Ratio (VVER), image-derived clod-size distribution (CSD), and Edge-Density Roughness Index (EDRI). These variables were selected because they represent three different aspects of ploughing quality: inversion, fragmentation, and surface condition.

TABLE (1): IMAGE-DERIVED VARIABLES USED IN THE PILOT WORKFLOW.

| **Variable** | **Abbreviation** | **Interpretation** |
|---|---|---|
| Visible Vegetation Exposure Ratio | VVER | Proxy for apparent soil inversion |
| Image-derived clod-size distribution | CSD | Proxy for soil fragmentation |
| Edge-density roughness index | EDRI | Proxy for surface structural irregularity |

*2.6 Visible Vegetation Exposure Ratio*

Visible vegetation exposure was used as a proxy indicator of apparent soil inversion. Images were converted from RGB/BGR to HSV color space because HSV is useful for separating color information from brightness variation. Green vegetation pixels were segmented using fixed HSV threshold values. Morphological opening and closing operations were then applied to reduce small noise pixels and improve mask continuity.

$$VVER = (N_{green} / N_{total}) \times 100$$

*University of Thi-Qar Journal of agricultural research*

*Thi-Qar Journal of agricultural research*

*ISSN Onlin:2708-9347, ISSN Print: 2708-9339 Volume 15, Issue 1 (2026) PP 229-242*

*https://jam.utq.edu.iq/index.php/main* https://doi.org/10.54174/0kgmcw24

where N_green is the number of detected green vegetation pixels and N_total is the total number of image pixels. This variable represents visible green vegetation remaining on the soil surface. It does not measure total buried biomass or non-green residue. Therefore, it was interpreted only as a proxy indicator of apparent inversion.

*2.7 Clod-size proxy analysis*

Soil clod features were extracted using an edge-and-contour-based method. Each image was converted to grayscale. Gaussian smoothing was applied to reduce noise while preserving major structural boundaries. The Canny edge detector was then used to identify edges associated with clod boundaries, cracks, and surface structural features. The Canny detector is a standard edge-detection method based on detection and localization criteria for identifying edge points in digital images (Canny, 1986).

External contours were extracted from the edge image, and very small contours were removed using a minimum area threshold to reduce noise. The area of each detected contour was used to calculate an equivalent circular diameter:

$$D = 2 \times \mathrm{sqrt}(A / \pi)$$

where D is the equivalent clod diameter in pixels and A is the detected contour area in pixels$^2$. Percentile indicators D10, D50, and D90 were calculated from the equivalent diameter distribution. Relative clod classes were defined as fine ($D < D50$),

medium ($D50 \leq D \leq D90$), and coarse ($D > D90$). Because these classes were percentile-based, they represent relative image-derived classes within this dataset and should not be interpreted as universal agronomic clod-size classes or absolute physical clod-size measurements.

*2.8 Edge-density surface structural roughness index*

Surface structural roughness was estimated using an edge-density index. Each image was converted to grayscale, and Canny edge detection was applied. The number of edge pixels was divided by the total number of pixels:

$$EDRI = N_{edge} / N_{total}$$

where N_edge is the number of detected edge pixels and N_total is the total number of image pixels. This index represents image texture complexity and visible surface structural irregularity. It should not be interpreted as true vertical soil surface roughness. Conventional soil roughness studies often rely on elevation-based methods such as profilometry, laser scanning, terrestrial laser scanning, stereo vision, or photogrammetric 3D reconstruction (Huang & Bradford, 1992; Darboux & Huang, 2003; Gilliot et al., 2017; Azizi et al., 2021).

*2.9 Data integration and visualization*

For each image, vegetation exposure, clod-size indicators, relative clod classes, and edge-density roughness index were calculated. Results were exported into separate CSV files and then merged into a final integrated dataset. Graphical outputs included vegetation masks, vegetation overlays, clod edge maps, filtered clod contours, clod-size histograms, clod class distribution charts, and roughness-index plots.

*2.10 Preliminary visual consistency check*

Because field re-sampling and laboratory validation were not available at this stage, a preliminary visual consistency check was used. Image-derived outputs were compared with structured visual interpretation of inversion, fragmentation, and roughness. This step was intended only to assess whether computational outputs aligned with expected visual field interpretation. It should not be considered formal validation. Future research should include independent expert scoring and physical validation using calibrated scale references, sieve analysis, soil moisture data, profilometry, LiDAR, stereo vision, or close-range photogrammetric reconstruction (Gilliot et al., 2017; Fanigliulo et al., 2020; Chen et al., 2024).

*University of Thi-Qar Journal of agricultural research*

*Thi-Qar Journal of agricultural research*

*ISSN Onlin:2708-9347, ISSN Print: 2708-9339 Volume 15, Issue 1 (2026) PP 229-242*

*https://jam.utq.edu.iq/index.php/main* https://doi.org/10.54174/0kgmcw24

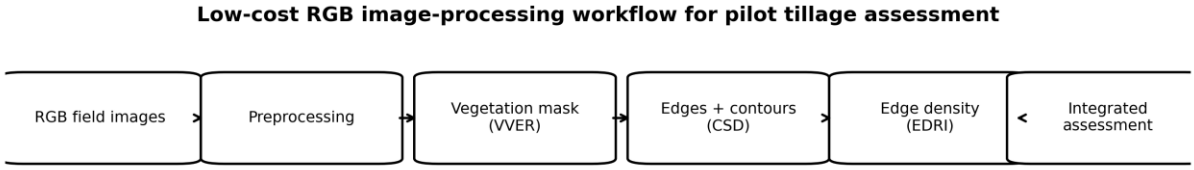


*Figure 1. Overview of the RGB image-processing workflow used to derive proxy indicators of soil inversion, clod-size distribution, and surface structural roughness.*

## III. RESULTS

*3.1 Visible vegetation exposure*

The mean visible vegetation exposure across the ten images was approximately 1.96%. This low value indicates limited visible green vegetation remaining on the soil surface after ploughing. As a proxy indicator, this suggests effective apparent soil inversion and burial of green vegetation within the analyzed image set.

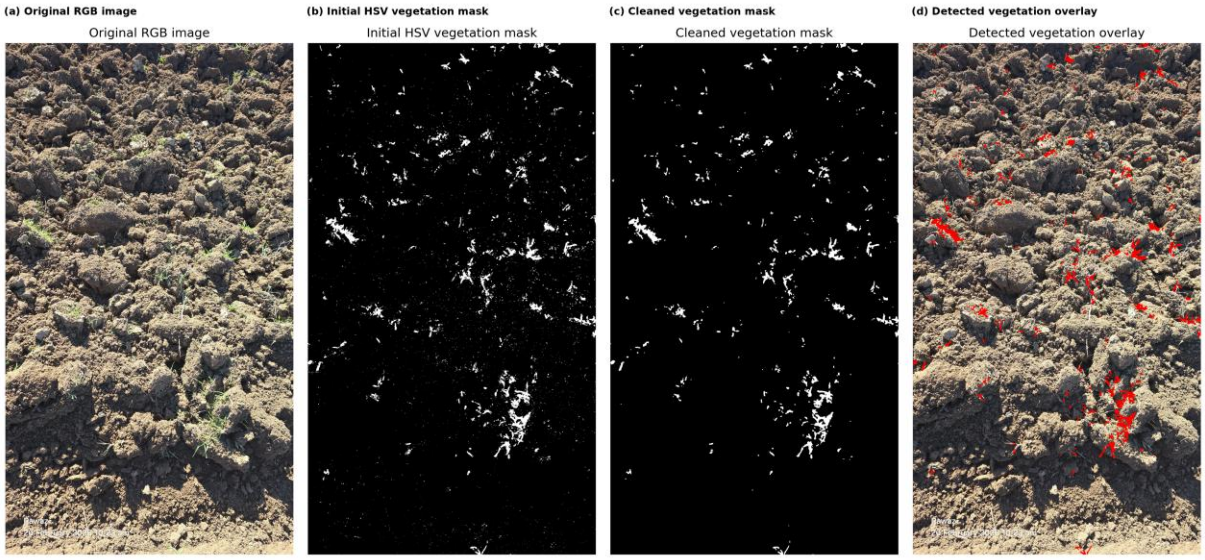


*Figure 2. Vegetation detection workflow: (a) original RGB image, (b) initial HSV-based vegetation mask, (c) morphologically cleaned mask, and (d) overlay highlighting detected vegetation. Vegetation coverage was computed as the ratio of detected green pixels to total image pixels.*

*University of Thi-Qar Journal of agricultural research*

*Thi-Qar Journal of agricultural research*

*ISSN Onlin:2708-9347, ISSN Print: 2708-9339 Volume 15, Issue 1 (2026) PP 229-242*

*https://jam.utq.edu.iq/index.php/main* https://doi.org/10.54174/0kgmcw24

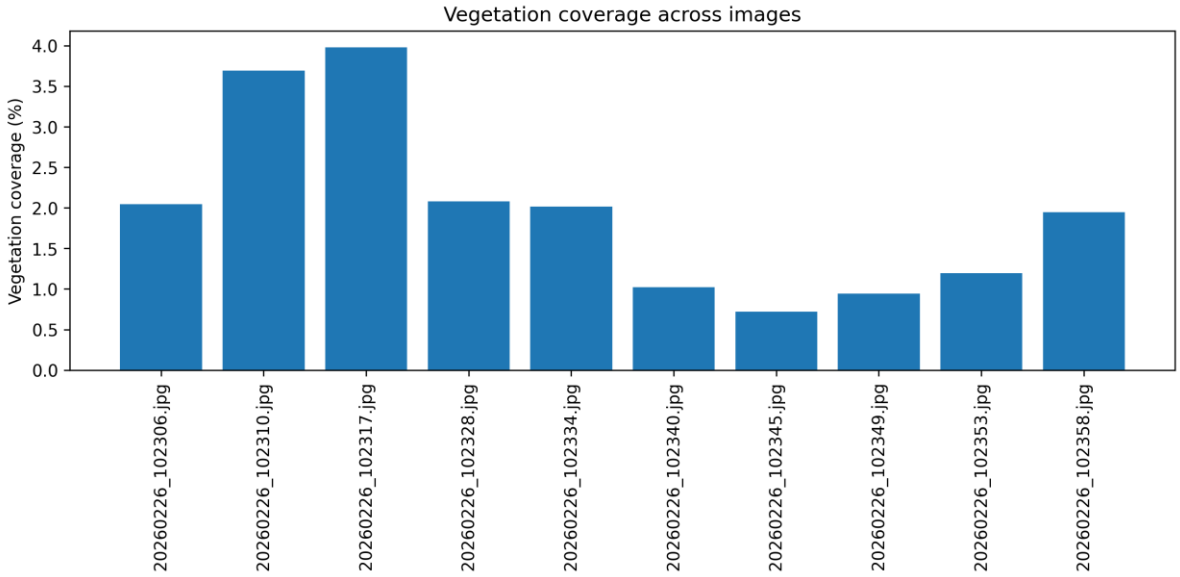


*Figure 3. Visible vegetation exposure across the analyzed images, used as a proxy indicator of apparent soil inversion quality.*

Table (2): Summary of image-derived soil surface indicators.

| Indicator | Mean result | Unit | Interpretation |
|---|---|---|---|
| Visible Vegetation Exposure Ratio (VVER) | 1.964 | % | Low visible vegetation; good apparent inversion |
| Detected clods per image | 495.500 | count | High structural segmentation of the visible soil surface |
| D10 | 12.164 | px | Lower-percentile image-derived clod-size proxy |
| D50 | 17.063 | px | Median image-derived clod-size proxy |
| D90 | 37.185 | px | Upper-percentile image-derived clod-size proxy |
| Fine class | 49.850 | % | Relative fine class within the image-derived dataset |
| Medium class | 40.081 | % | Relative medium class within the image-derived dataset |
| Coarse class | 10.069 | % | Relative coarse class within the image-derived dataset |
| Edge-density roughness index (EDRI) | 0.301 | ratio | High image structural complexity typical of primary tillage |

*Clod-size proxy indicators*

The image-derived clod analysis showed stable percentile-based clod-size patterns across the image set. The mean D50 value was approximately 17.06 pixels, indicating a moderate median image-derived clod-size proxy. The relative class distribution was dominated by fine and medium features, while the upper 10% of detected clod features formed the coarse class.

*University of Thi-Qar Journal of agricultural research*

*Thi-Qar Journal of agricultural research*

*ISSN Onlin:2708-9347, ISSN Print: 2708-9339 Volume 15, Issue 1 (2026) PP 229-242*

*https://jam.utq.edu.iq/index.php/main* https://doi.org/10.54174/0kgmcw24

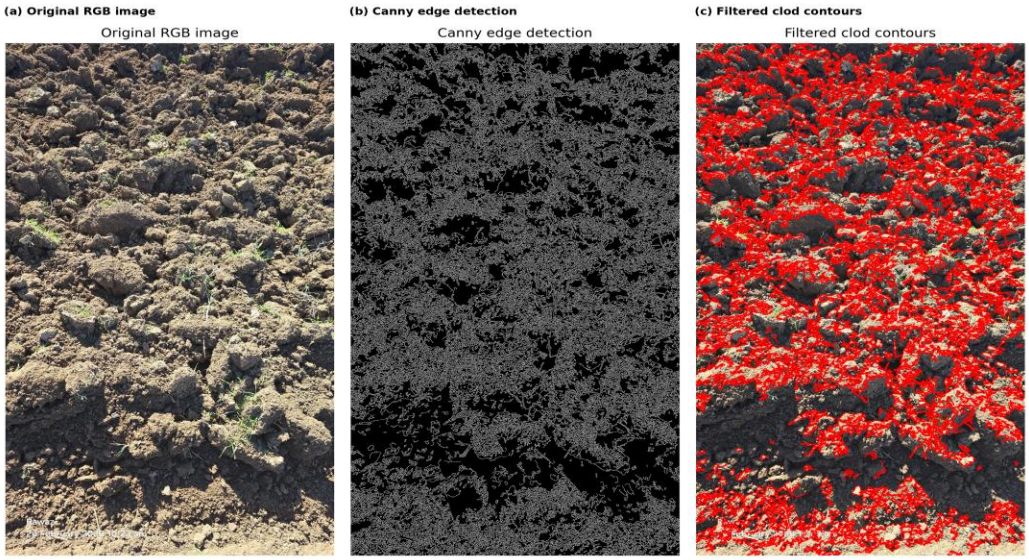


Figure 4. Clod detection procedure: (a) original RGB image, (b) edge detection using the Canny operator, and (c) filtered contours representing detected soil aggregates after removal of small noise components.

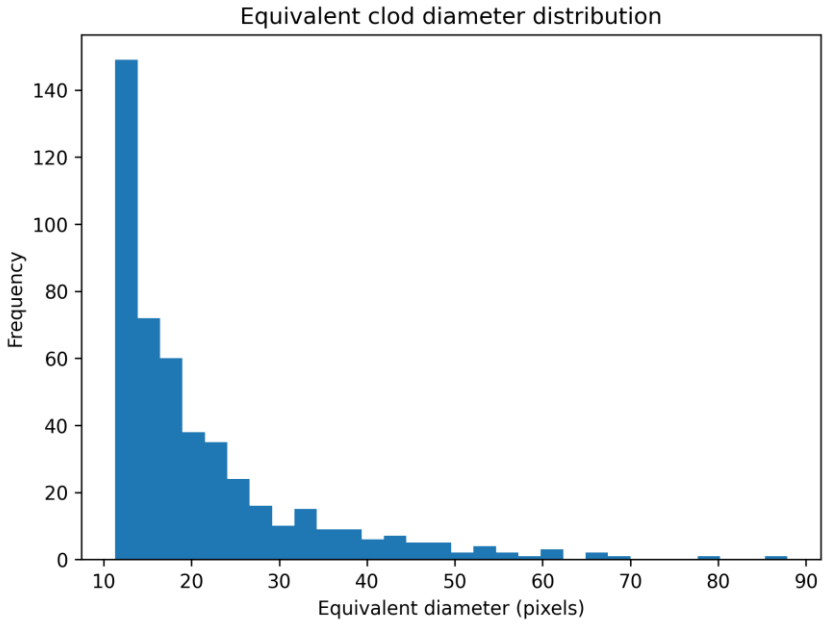


*Figure 5. Distribution of equivalent clod diameters, expressed in pixels, for a representative image. Percentile-based indicators D10, D50, and D90 were used to describe the clod-size distribution.*

*University of Thi-Qar Journal of agricultural research*

*Thi-Qar Journal of agricultural research*

*ISSN Onlin:2708-9347, ISSN Print: 2708-9339 Volume 15, Issue 1 (2026) PP 229-242*

*https://jam.utq.edu.iq/index.php/main* https://doi.org/10.54174/0kgmcw24

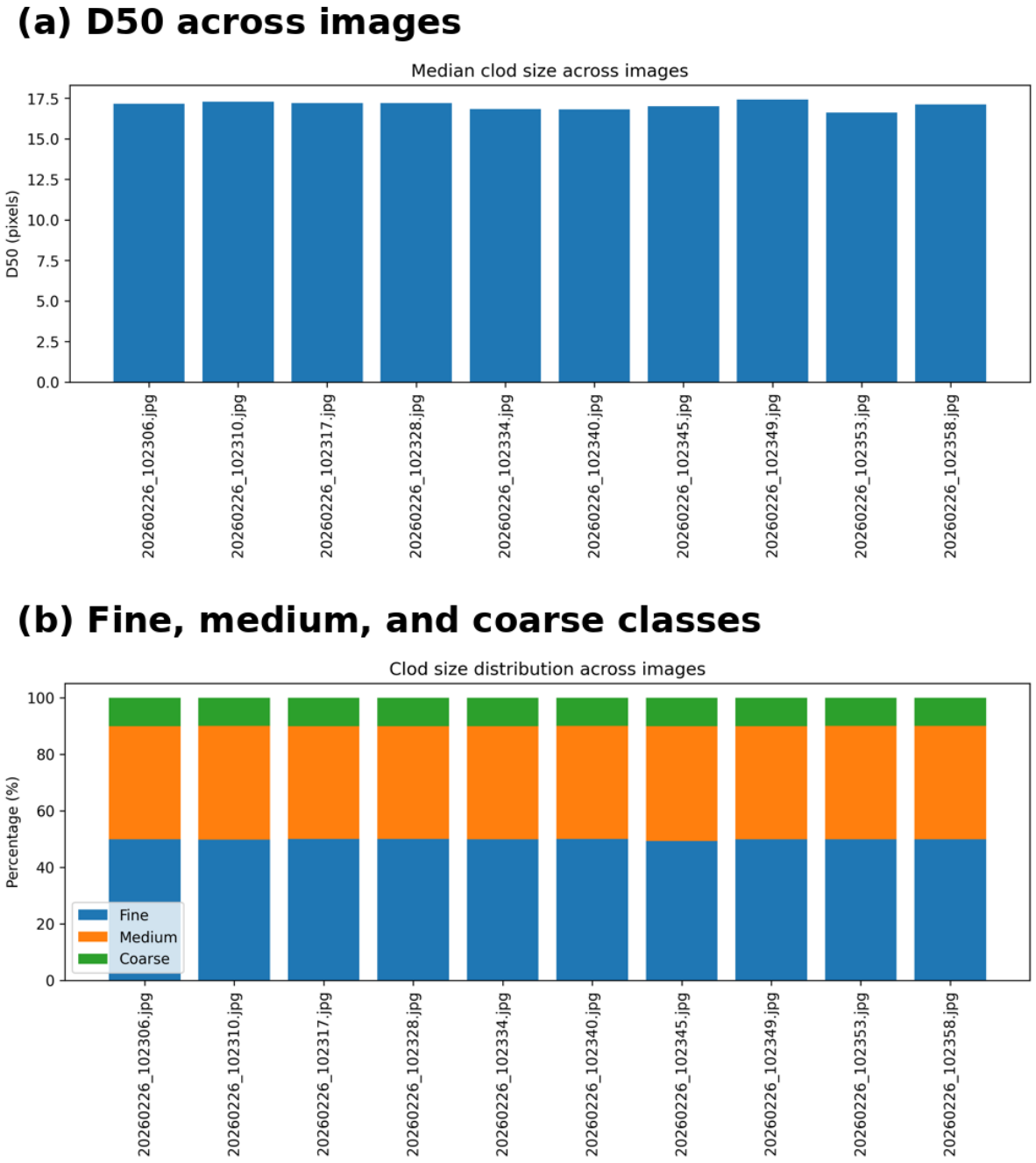


*Figure 6. Clod-size results across the ten analyzed images: median clod size (D50) and percentage distribution of fine, medium, and coarse clod classes. The results provide proxy indicators of post-plough soil fragmentation.*

*University of Thi-Qar Journal of agricultural research*

*Thi-Qar Journal of agricultural research*

*ISSN Onlin:2708-9347, ISSN Print: 2708-9339 Volume 15, Issue 1 (2026) PP 229-242*

*https://jam.utq.edu.iq/index.php/main* https://doi.org/10.54174/0kgmcw24

*3.3 Surface structural roughness*

The mean edge-density roughness index was approximately 0.301. This indicates high image texture complexity and a visibly irregular soil surface following ploughing. The edge-density result is consistent with a fresh primary tillage surface containing clod boundaries, cracks, voids, and irregular micro-relief features.

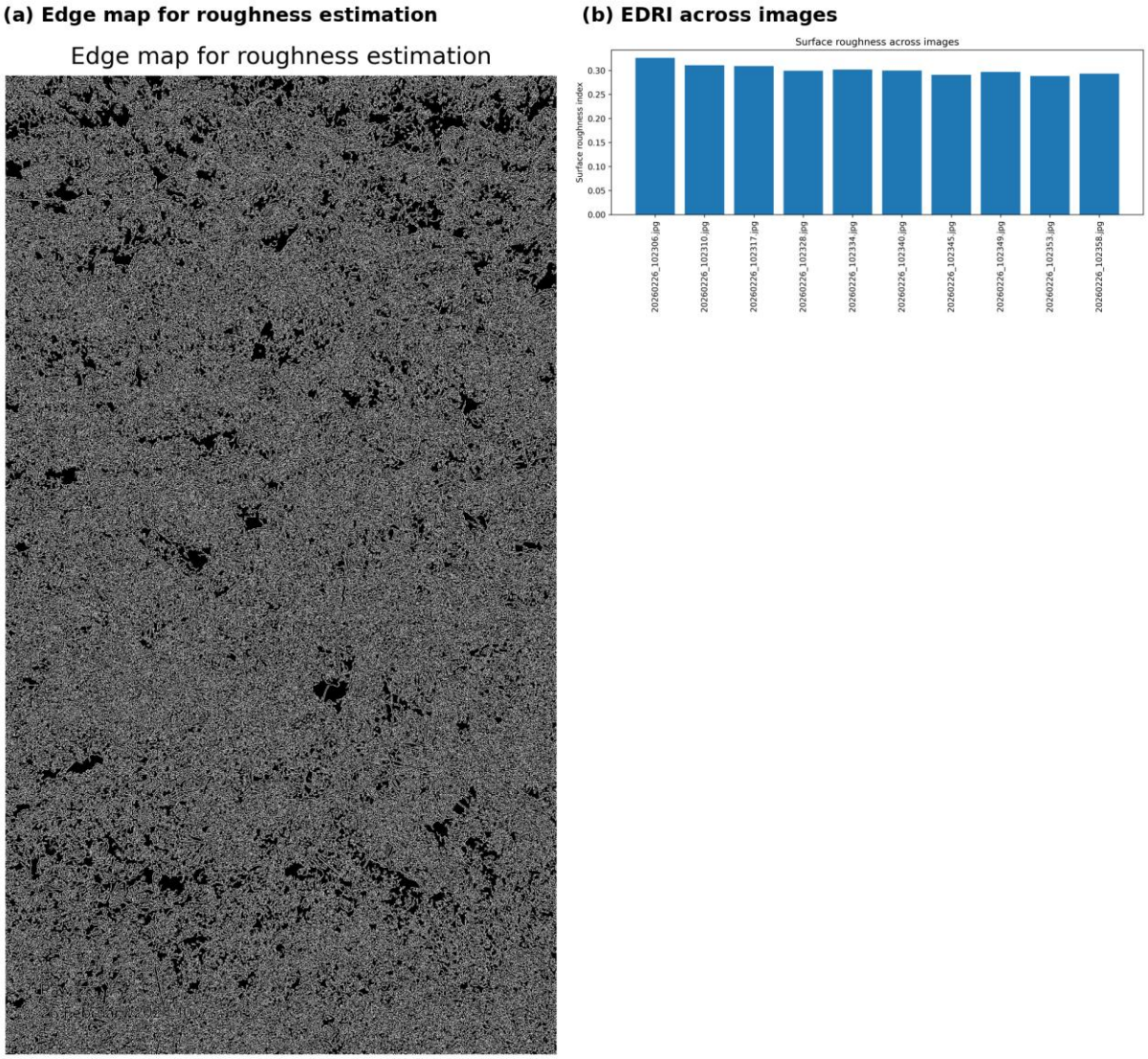


*Figure 7. Surface roughness estimation using edge density: (a) edge map derived from the Canny operator and (b) roughness index values across all images. The index represents the proportion of edge pixels to total image pixels.*

Table (3): Main image-processing parameters used in the pilot workflow.

*University of Thi-Qar Journal of agricultural research*

*Thi-Qar Journal of agricultural research*

*ISSN Onlin:2708-9347, ISSN Print: 2708-9339 Volume 15, Issue 1 (2026) PP 229-242*

*https://jam.utq.edu.iq/index.php/main* https://doi.org/10.54174/0kgmcw24

| Parameter | Value | Purpose |
|---|---|---|
| Vegetation color space | HSV | Used to separate green vegetation from soil tones |
| HSV lower threshold | [30, 25, 25] | Lower boundary for green detection |
| HSV upper threshold | [95, 255, 255] | Upper boundary for green detection |
| Morphological kernel | 3 × 3 | Opening and closing for vegetation mask cleaning |
| Gaussian blur | 5 × 5 | Noise reduction before clod edge detection |
| Canny thresholds | 50, 150 | Edge detection for clod and roughness analysis |
| Minimum contour area | 100 $px^2$ | Small noisy contours removed from clod analysis |
| Clod diameter equation | $D = 2 \times \sqrt{(A/\pi)}$ | Equivalent circular diameter in pixels |

*University of Thi-Qar Journal of agricultural research*

*Thi-Qar Journal of agricultural research*

*ISSN Onlin:2708-9347, ISSN Print: 2708-9339 Volume 15, Issue 1 (2026) PP 229-242*

*https://jam.utq.edu.iq/index.php/main* https://doi.org/10.54174/0kgmcw24

*3.4 Integrated per-image results*

Table (4): Integrated per-image results from the ten RGB field images.

| Image | VVER_% | Clods_n | D10_px | D50_px | D90_px | Fine_% | Medium_% | Coarse_% | EDRI |
|---|---|---|---|---|---|---|---|---|---|
| 20260226_102306.jpg | 2.046 | 477 | 12.127 | 17.150 | 37.236 | 49.895 | 40.042 | 10.063 | 0.326 |
| 20260226_102310.jpg | 3.690 | 517 | 12.453 | 17.279 | 37.147 | 49.710 | 40.232 | 10.058 | 0.311 |
| 20260226_102317.jpg | 3.981 | 512 | 12.021 | 17.205 | 39.078 | 50.000 | 39.844 | 10.156 | 0.309 |
| 20260226_102328.jpg | 2.082 | 466 | 12.270 | 17.196 | 40.508 | 50.000 | 39.914 | 10.086 | 0.299 |
| 20260226_102334.jpg | 2.013 | 507 | 12.127 | 16.831 | 35.588 | 49.901 | 40.039 | 10.059 | 0.302 |
| 20260226_102340.jpg | 1.024 | 498 | 12.250 | 16.803 | 36.843 | 50.000 | 39.960 | 10.040 | 0.300 |
| 20260226_102345.jpg | 0.720 | 497 | 11.995 | 17.001 | 38.087 | 49.296 | 40.644 | 10.060 | 0.291 |
| 20260226_102349.jpg | 0.942 | 523 | 12.179 | 17.426 | 35.979 | 49.904 | 39.962 | 10.134 | 0.297 |
| 20260226_102353.jpg | 1.195 | 527 | 12.143 | 16.622 | 33.904 | 49.905 | 40.038 | 10.057 | 0.288 |
| 20260226_102358.jpg | 1.947 | 431 | 12.074 | 17.113 | 37.484 | 49.884 | 40.139 | 9.977 | 0.293 |

*University of Thi-Qar Journal of agricultural research*

*Thi-Qar Journal of agricultural research*

*ISSN Onlin:2708-9347, ISSN Print: 2708-9339 Volume 15, Issue 1 (2026) PP 229-228*

*https://jam.utq.edu.iq/index.php/main* https://doi.org/10.54174/xsnz1j52

## IV. DISCUSSION

The results suggest that the three-body mouldboard plough achieved effective apparent inversion, as indicated by low visible vegetation exposure. This is consistent with the known function of mouldboard ploughs, which are designed to lift and invert soil slices and incorporate surface material. However, the result should be interpreted as visible vegetation exposure only, not total residue burial.

The clod-size proxy results showed moderate fragmentation. Although almost half of the detected clod features fell below the median diameter threshold, a substantial proportion remained in the medium class, and approximately 10% represented coarse image-derived features. This supports the interpretation that primary tillage produced effective soil disturbance but did not produce a fine seedbed. Tillage literature recognizes that soil fragmentation is influenced by soil mechanical behavior, implement geometry, and operating conditions (Koolen & Kuipers, 1983; Godwin, 2007; Godwin et al., 2007).

The roughness index indicated a highly textured and irregular surface. This is typical of primary tillage, where the objective is soil loosening and inversion rather than final seedbed refinement. Conventional soil roughness studies often use laser scanners, profile measurements, or 3D reconstruction methods to quantify surface elevation variation (Huang & Bradford, 1992; Darboux & Huang, 2003; Jester & Klik, 2005). In contrast, the present study used 2D edge density, which should be interpreted as a proxy for structural complexity rather than true topographic roughness.

A key finding of this pilot study is that effective inversion does not necessarily correspond to optimal fragmentation. The low visible vegetation exposure suggests good apparent inversion, while the clod-size and roughness indicators show that the soil surface remained moderately fragmented and rough. This distinction is important for tillage assessment because inversion, fragmentation, and seedbed refinement are controlled by different soil-tool interaction processes.

The workflow demonstrated practical value because it produced consistent outputs from ordinary RGB images. However, the method remains preliminary. It should be used as a comparative field-assessment tool rather than a replacement for calibrated physical methods. Stronger validation would require comparison with sieve-based aggregate analysis, calibrated physical scale references, laser/profilometer measurements, stereo vision, or photogrammetric 3D surface models (Gilliot et al., 2017; Azizi et al., 2021; Chen et al., 2024).

### *4.1 Potential for low-cost drone-based use*

A major practical implication of this pilot study is its potential transferability to low-cost drone-based field monitoring. The present workflow was tested using close-range smartphone RGB images, but the same principles could be adapted to UAV imagery captured from low altitude. A drone-based workflow could allow larger field coverage, more systematic sampling, and spatial mapping of post-plough soil condition. Previous research has demonstrated the use of light drone 3D imaging for assessing tillage-quality parameters such as roughness and cloddiness, while UAS imagery has also been applied to crop residue cover estimation (Fanigliulo et al., 2020; Upadhyay et al., 2022; Azimi et al., 2024). Therefore, future work could extend the proposed workflow by acquiring nadir UAV images over multiple plots, generating spatial maps of vegetation exposure, clod-size proxies, and edge-density roughness, and comparing these outputs with ground-truth physical measurements.

## V. CONCLUSIONS

This pilot study demonstrated that RGB image processing can provide practical proxy indicators for evaluating soil surface condition after three-body mouldboard ploughing. The workflow produced three

*ISSN Onlin:2708-9347, ISSN Print: 2708-9339 Volume 15, Issue 1 (2026) PP 229-228*

*https://jam.utq.edu.iq/index.php/main* https://doi.org/10.54174/xsnz1j52

useful outputs: visible vegetation exposure, relative clod-size distribution, and edge-density surface structural roughness.

The analyzed images showed low visible vegetation exposure, suggesting effective apparent inversion. However, clod-size and roughness indicators showed that the soil remained moderately fragmented and structurally rough. This indicates that the plough performed effectively as a primary tillage implement but that secondary tillage would likely be required for finer seedbed preparation.

This pilot study also provides a foundation for future low-cost drone-based tillage assessment. When combined with UAV image acquisition, the proposed workflow could support spatial mapping of soil inversion, fragmentation, and surface structural roughness across larger field areas. However, future drone-based applications should include physical calibration, ground-control points, controlled flight height, nadir imaging, and validation against conventional clod-size and roughness measurements.

## VI. REFERENCES

Azimi, F., & Jung, J. (2024). Automated crop residue estimation via unsupervised techniques using high-resolution UAS RGB imagery. *Remote Sensing, 16*(7), 1135. https://doi.org/10.3390/rs16071135

Azizi, A., Abbaspour-Gilandeh, Y., Vannier, E., Dusséaux, R., Mseri-Gundoshmian, T., & Moghaddam, H. A. (2021). Estimation of soil surface roughness using stereo vision approach. *Sensors, 21*(13), 4386. https://doi.org/10.3390/s21134386

Bögel, T., Osinenko, P., & Herlitzius, T. (2016). Assessment of soil roughness after tillage using spectral analysis. *Soil and Tillage Research, 159*, 73–82. https://doi.org/10.1016/j.still.2016.02.004

Bogrekci, I., & Godwin, R. J. (2007). Development of an image-processing technique for soil tilth sensing. *Biosystems Engineering, 97*(3), 323–331. https://doi.org/10.1016/j.biosystemseng.2007.03.025

Bradski, G. (2000). The OpenCV Library. *Dr. Dobb's Journal of Software Tools, 25*(11), 120–125. No DOI found / generally cited without DOI.

Canny, J. (1986). A computational approach to edge detection. *IEEE Transactions on Pattern Analysis and Machine Intelligence, PAMI-8*(6), 679–698. https://doi.org/10.1109/TPAMI.1986.4767851

Chen, X., Guo, Y., Hu, J., Xu, G., Liu, W., Ma, G., Ding, Q., & He, R. (2024). Quantitative evaluation of post-tillage soil structure based on close-range photogrammetry. *Agriculture, 14*(12), 2124. https://doi.org/10.3390/agriculture14122124

Darboux, F., & Huang, C. H. (2003). An instantaneous-profile laser scanner to measure soil surface microtopography. *Soil Science Society of America Journal, 67*, 92–99. https://doi.org/10.2136/sssaj2003.9200

Dusséaux, R., & Vannier, E. (2022). Soil surface roughness modelling with the bidirectional autocorrelation function. *Biosystems Engineering, 220*, 87–102. https://doi.org/10.1016/j.biosystemseng.2022.05.012

Eltner, A., Kaiser, A., Castillo, C., Rock, G., Neugirg, F., & Abellán, A. (2016). Image-based surface reconstruction in geomorphometry: Merits, limits and developments. *Earth Surface Dynamics, 4*, 359–389. https://doi.org/10.5194/esurf-4-359-2016

*ISSN Onlin:2708-9347, ISSN Print: 2708-9339 Volume 15, Issue 1 (2026) PP 229-228*

*https://jam.utq.edu.iq/index.php/main* https://doi.org/10.54174/xsnz1j52

FAO. (2008). *Visual Soil Assessment: Field Guide*. Food and Agriculture Organization of the United Nations. No DOI found / institutional guide.

Gilliot, J. M., Vaudour, E., & Michelin, J. (2017). Soil surface roughness measurement: A new fully automatic photogrammetric approach applied to agricultural bare fields. *Computers and Electronics in Agriculture, 134*, 63–78. https://doi.org/10.1016/j.compag.2017.01.010.

Godwin, R. J. (2007). A review of the effect of implement geometry on soil failure and implement forces. *Soil and Tillage Research, 97*(2), 331–340. https://doi.org/10.1016/j.still.2006.06.010

Godwin, R. J., O'Dogherty, M. J., Saunders, C., & Balafoutis, A. T. (2007). A force prediction model for mouldboard ploughs incorporating the effects of soil characteristic properties, plough geometric factors and ploughing speed. *Biosystems Engineering, 97*, 117–129. https://doi.org/10.1016/j.biosystemseng.2007.02.001

Huang, C., & Bradford, J. M. (1992). Applications of a laser scanner to quantify soil microtopography. *Soil Science Society of America Journal, 56*, 14–21. https://doi.org/10.2136/sssaj1992.03615995005600010002x

Jester, W., & Klik, A. (2005). Soil surface roughness measurement—methods, applicability, and surface representation. *Catena, 64*(2–3), 174–192. https://doi.org/10.1016/j.catena.2005.08.005

Koolen, A. J., & Kuipers, H. (1983). *Agricultural Soil Mechanics*. Springer. https://doi.org/10.1007/978-3-642-69010-5

Spoor, G. (2006). Alleviation of soil compaction: Requirements, equipment and techniques. *Soil Use and Management, 22*, 113–122. https://doi.org/10.1111/j.1475-2743.2006.00015.x

Upadhyay, P. C., Lory, J. A., DeSouza, G. N., Lagaunne, T. A. P., & Spinka, C. M. (2022). Classification of crop residue cover in high-resolution RGB images using machine learning. *Journal of the ASABE, 65*(1), 75–86. https://doi.org/10.13031/ja.14572